Available online at www.sciencedirect.com
ScienceDirect
Chinese Journal of Natural Medicines 2021, **19**(7): 528-535
doi: 10.1016/S1875-5364(21)60052-3
Chinese Journal of Natural Medicines

•Research article•

Germacranolide sesquiterpenes from *Carpesium cernuum* and their anti-leukemia activity

YAN Chen[1, 2Δ], LONG Qun[2, 3Δ], ZHANG Yun-Dong[1], BABU Gajendran[2, 3], KRISHNAPRIYA Madhu Varier[4], QIU Jian-Fei[2, 3], SONG Jing-Rui[2, 3], RAO Qing[2, 3], YI Ping[2, 3], SUN Mao[1, 2*], LI Yan-Mei[2, 3*]

[1] *Department of Pharmacy, An Shun City People's Hospital, Anshun 561000, China;*
[2] *Key Laboratory of Chemistry for Natural Products of Guizhou Province and Chinese Academic of Sciences, Guiyang 550014, China;*
[3] *State Key Laboratory of Functions and Applications of Medicinal Plants, Guizhou Medical University, Guiyang 550014, China;*
[4] *Department of Medical Biochemistry, Dr. ALM PGIBMS, University of Madras, Taramani Campus, Chennai, India*

Available online 20 Jul., 2021

[ABSTRACT] In this study, three new germacranolide sesquiterpenes (**1**–**3**), together with six related known analogues (**4**–**9**) were isolated from the whole plant of *Carpesium cernuum*. Their structures were established by a combination of extensive NMR spectroscopic analysis, HR-ESIMS data, and ECD calculations. The anti-leukemia activities of all compounds towards three cell lines (HEL, KG-1a, and K562) were evaluated in *vitro*. Compounds **1**–**3** exhibited moderate cytotoxicity with IC_{50} values ranging from 1.59 to 5.47 μmol·L^{-1}. Mechanistic studies indicated that **2** induced apoptosis by decreasing anti-apoptotic protein Bcl-2 and activating the caspase family in K562 cells. These results suggest that compound **2** is a potential anti-leukemia agent.

[KEY WORDS] *Carpesium cernuum*;; Germacranolides;; Anti-leukemia; K562; MAPK
[CLC Number] R284, R965 **[Document code]** A **[Article ID]** 2095-6975(2021)07-0528-08

Introduction

Germacranolides are a type of germacrene sesquiterpene lactone that contain a unique ten-membered carbocyclic skeleton fused with a five-membered γ-lactone [1]. With a broad range of biological activities as well as complex and diverse stereo configurations, germacrene sesquiterpenes have attracted significant attention and research interest [2-4]. For exmaple, parthenolide from *Tanacetum parthenium* has clear potential for in *vivo* anti-leukemia action and is currently evaluated under Phase II clinical trial [5-6].

Sesquiterpenes, flavonoids, and phenols isolated from Asteraceae family plants possess a broad spectrum of biological and pharmacological properties. For instance, extracts derived from *Gochnatia hypoleuca*, *Verbesina virginica*, *Melampodium leucanthum* and *Achillea wilhelmsii* (Asteraceae), exert anti-proliferative activity towards prostate cancer PC-3 and DU145 cell lines [7-9]. In many cases, the sesquiterpenes lactones produce cytotoxicity by telomerase reverse transcriptase inhibition [10]. Furthermore, tricyclic sesquiterpenes and germacranolide sesquiterpene lactones arrest K562 cells at the mitotic phase, forming abnormal mitotic spindles [8].With respect to these chemotherapeutic effects, the Asteraceae family is of great research interest.

The genus *Carpesium* (Asteraceae), with approximately 21 species, is widely distributed throughout Central Asia; from this group comes a large number of monoterpenes, dimeric sesquiterpenoids, and germacranolide sesquiterpenes with highly oxygenated systems and a broad array of biological activities [1-3]. Previous investigations into this genus have led to the isolation of germacrene sesquiterpene lactones from *C. cernuum* [11] that inhibited cell adhesion in MDA-MB-231 cells at its lowest IC_{50} concentration and caused apoptosis. This even influenced cell migration through attenuation of MMP9, TIMP1, COL4A2, and CD44 [12]. Moreover, a silver nanoparticle synthesized from

[Received on] 06-Mar.-2021
[Research funding] This work was supported by the Science and Technology Department of Guizhou Province (No. QKHJC[2016]1002, 81872772, 81960546, and U1812403), the National Natural Science Foundation of China (Nos. 81872772, 81960546, and U1812403), the Science and Technology Department of Anshun City (No. ASKP[2019]3), and the 100 Leading Talents of Guizhou Province (fund for LI Yan-Mei, Nos. P2018-KF11 and QZYY-019-022).
[*]**Corresponding author]** E-mails: sunmaohaohao@163.com (SUN Mao); liyanmei518@hotmail.com (LI Yan-Mei)
[Δ]These authors contributed equally to this work.
These authors have no conflict of interest to declare.

the extract of *C. cernuum* reduced the cellular adhesion on *Mus musculus* skin melanoma cells (B16F10) and human lung cancer cells (A549) in a dose-dependent manner [13]. However, the cytotoxic activity of *C. cernuum* extracts or its constituents on leukemia cells are still unclear. Recently, our reserach group reported two sesquiterpene lactones, carpescernolides A and B, isolated from *C. cernuum*, with two unusual oxygen bridges [14]. In our continuing search for biologically active constituents, a detailed investigation of *C. cernuum* was carried out, where three new germacrene sesquiterpene lactones, carpescernolides (**1**–**3**), along with six known compounds (**4**–**9**) were isolated from an entire plant of *C. cernuum* and screened for anti-leukemic activity (Fig. 1).

Results and Discussion

Structure elucidation of the compounds

Carpescernolide C was obtained as a white amorphous powder. Its molecular formula, $C_{19}H_{26}O_7$, was established by ^{13}C NMR and HR-ESIMS (*m/z* 389.1570 $[M + Na]^+$, Calcd. for $C_{19}H_{26}O_7Na$, 389.1571) data. The IR spectrum suggests the presence of hydroxyl (3439 cm^{-1}) and carbonyl (1767 cm^{-1}) groups as well as the presence of double bonds (1632 cm^{-1}). The ^1H NMR spectrum displayed signals for four methyl groups (δ_H 1.25, 1.24, 1.24, 1.09) and two exocyclic olefinic protons (δ_H 6.09, d, J = 2.4 Hz; 6.16, d, J = 2.4 Hz). In the HMBC spectrum (Fig. 2a), two methyls at δ_H 1.25 (d, J = 5.6 Hz) and 1.23 (d, J = 5.6 Hz) showed long-range correlations to the carbonyl carbon at δ_C 177.6, suggesting the presence of an isobutyloxy group. The remaining 15 carbon resonances indicated a sesquiterpenoid skeleton except for the substituent. The 10-membered ring inferred from the ^1H–^1H COSY spectrum (Fig. 2a), H_3-14/H-10/H_2-1/H-2/H_2-3 and H-5/H-6/H-7/H-8, together with the HMBC correlations

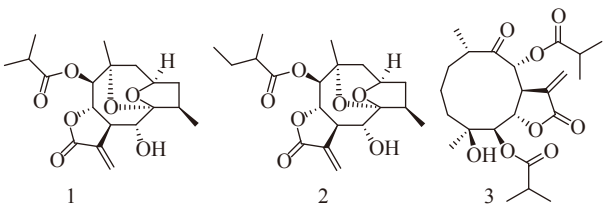

Fig. 1 Chemical structures of compounds 1–3

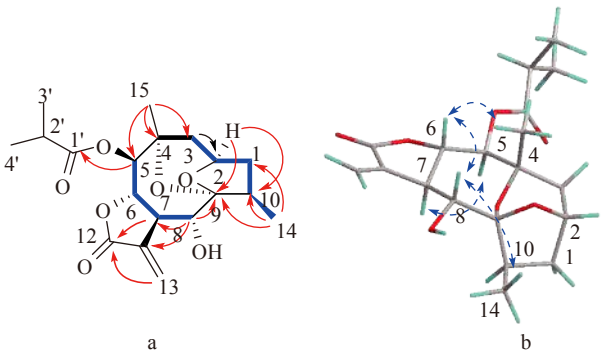

Fig. 2 (a) Key HMBC (H→C) and ^1H–^1H COSY (—) correlations of 1; (b) Selected ROESY correlations (H↔H) of 1

from H_3-14 (δ_H 1.09) to C-1 (δ_C 40.0), C-9 (δ_C 107.9), and C-10 (δ_C 36.9); from H-2 (δ_C 4.60) to C-9 (δ_C 107.9) and C-10 (δ_C 36.9); from H_3-15 (δ_H 1.25) to C-4 (δ_C 73.3), C-3 (δ_C 47.6), and C-5 (δ_C 81.0) as well as H-8 (δ_H 3.80) to C-7 (δ_C 50.8), C-9 (δ_C 107.9), and C-11 (δ_C 140.4) were observed. In addition, Me-14 and Me-15 were bound to C-10 and C-4, respectively. An *α*-methylene-*γ*-lactone moiety was established by the presence of the two doublets of H-13a at δ_H 6.16 (J = 2.4 Hz) and H-13b at δ_H 6.09 (J = 2.4 Hz) as shown in Table 1, and C-12 at δ_C 170.6, C-11 at δ_C 140.4 and methylene C-13 at δ_C 120.9 as shown in Table 2, which was further confirmed by HMBC correlations from H-7 and H_2-13 to C-12 and from H-8 to C-11. The key HMBC correlation from H-

Table 1 ^1H NMR data for 1–3 (400 MHz, *J* in Hz)

Position	1[a]	2[a]	3[b]
1*α*	2.56, m	2.52 m	1.98, m
1*β*	1.33, m	1.28, m	1.34, m
2	4.60, td (1.4, 6.4)	4.56, td (1.4, 6.4)	0.97, m (*α*)
	-	-	0.85, m (*β*)
3*α*	2.64, m	2.57, m	1.88, m
3*β*	1.61, d (10.8)	1.57, d (10.8)	1.61, m
4	-	-	-
5	5.59, d (8.0)	5.57, d (8.0)	4.87,s
6	4.43, t (8.4)	4.37, t (8.4)	5.11, d (4.8)
7	3.31, m	3.28, m	3.41, m
8	3.80, d (8.0)	3.74, d (8.0)	5.05, d (10.8)
9	-	-	-
10	2.31, m	2.26, m	3.12, (m)
11	-	-	-
12	-	-	-
13a	6.16, d (2.4)	6.16, d (2.4)	6.39 d (2.4)
13b	6.09, d (2.4)	6.09, d (2.4)	5.95, d (2.4)
14	1.09, d (5.2)	1.04, d (5.6)	1.29, d (6.8)
15	1.24, s	1.20, s	1.10, s
1′	-	-	-
2′	2.65, m	2.43, m	2.62, m
3′	1.25, d (5.6)	1.52, m; 1.72, m	1.15, m
4′	1.23, d (5.6)	0.95, t (6.0)	1.15, m
5′	-	1.17, d (6.4)	-
1″			-
2″			2.62, m
3″			1.15, m
4″			1.15, m

[a] measured in CD_3OD; [b] measured in $CDCl_3$

5 (δ_H 5.59, d, J = 8.0 Hz) to the carbonyl carbon (δ_C 177.6) of the isobutyloxy group suggested that the substituent group was located at C-5. The characteristic chemical shifts of C-2, C-4, and C-9 along with two unassigned degrees of saturation implied the presence of the oxygen bridges of C-2-C-9 and C-4-C-9, which was further established by comparision of chemical shifts of this compound with those of ineupatolide E [15]. Its relative configuration was inferred from a ROESY spectrum (Fig. 2b). The correlations observed for H-2/H-1α, H-6/H-8, H-8/Me-14, Me-15/H-6, H-5/H-3α, and H-5/H-7 indicated the orientations of H-2 (α), H-5 (α), H-6 (β), H-7 (α), H-8 (β), H-10 (α), Me-14 (β) and Me-15 (β), respectively. The findings mentioned above indicated that **1** was very similar to ineupatolide E [15]. The only difference was that an isobutyloxy group was attached to the C-5 position in compound **1** instead of the angelate group observed in ineupatolide E. The absolute configuration of **1** was finally assigned by calculated results from electronic circular dichroism (ECD) spectra using time-dependent density functional theory with Gaussian09. The calculated ECD of **1** matched well with the experimentally recorded ECD spectra (Fig. 3) (Fig. S30, Supporting Information). So, the absolute configuration was established as shown in Fig. 1. Therefore, the structure of carpescernolide C (**1**) was established as 2, 9-epoxy-4, 9-epoxy-8-hydroxy-5-(isobutyloxy) germacran-6, 12-olide.

Table 2 ^{13}C NMR data for **1**–**3** (100 MHz, J in Hz)

Position	**1**[a]	**2**[a]	**3**[b]
1	40.0	40.0	32.1
2	73.3	73.3	19.0
3	47.6	47.6	35.4
4	72.3	72.3	74.3
5	81.0	80.9	75.7
6	78.7	78.6	71.5
7	50.8	50.8	45.6
8	69.5	69.5	76.9
9	107.9	107.9	210.4
10	36.9	36.9	44.7
11	140.4	140.4	133.7
12	170.6	171.2	168.8
13	120.9	120.8	127.3
14	13.4	13.4	19.72
15	24.6	24.6	24.3
1′	177.6	177.1	175.5
2′	35.4	42.6	33.5
3′	19.3	27.7	18.6
4′	19.2	11.9	18.6
5′	-	13.4	-
1″			176.3
2″			34.0
3″			18.8
4″			18.8

[a] measured in CD_3OD; [b] measured in $CDCl_3$

The HR-ESIMS data of carpescernolide D (**2**) suggested a molecular formula of $C_{20}H_{28}O_7$. A comparison of the NMR spectra (Tables 1−2) of **2** with those of **1** showed they have very similar structures where the only difference was that the 2-methylpropanoyloxy group in **1** was substituted by a 2-methylbutanoyloxy group in **2**. The HMBC correlations of H-5 (δ_H 5.57) with C-1′ (δ_C 177.1), of H-2′ (δ_H 2.65, m) with C-1′, C-2′ (δ_C 41.1), C-3′ (δ_C 26.4), C-4 (δ_C 11.5)′, and C-5′ (δ_C 13.1) indicated the 2-methylbutanoyloxy group was located at C-5 (Fig. S31, Supporting Information). The relative configuration of **2** was almost the same as those of **1**. The absolute configuration of **2** was assigned by comparing the ECD with that of **1** and analyzing the same biosynthesis pathway with **1**. Therefore, the absolute configuration was established as shown in Fig. 1. Therefore, compound **2**, carpescernolide D, was established as 2, 9-epoxy-4, 9-epoxy-8-hydroxy-9-(2-methylbutanoyloxy) germacran-6,12-olide.

Carpescernolide E (**3**), a white powder, has a molecular formula of $C_{23}H_{34}O_8$, which was deduced from the HR-ESIMS at m/z 461.2147 $[M + Na]^+$ (Calcd. for $C_{23}H_{34}O_8Na$, 461.2146) and consistent with its NMR data (Tables 1−2). Strong IR absorptions at 3444, 1737 and 1639 cm^{-1} showed the presence of hydroxyl and carbonyl groups as well as double bonds, respectively. The ^{1}H and ^{13}C NMR (DEPT) spectra of **3** showed an α-methylene-γ-lactone at δ_H 6.39 (1H, d, J = 2.4 Hz, H_a-13) and 5.95 (1H, d, J = 2.4 Hz, H_b-13), δ_C 133.7 (C-11), 127.3 (C-13) and 168.8 (C-12); a ketone group at δ_C 210.4 (C-9); and an oxygenated quaternary carbon at δ_C 74.3 (C-4). The remaining data indicated the presence of two methyl groups, three methylenes, three oxygenated methines at δ_H 4.87 (1H, s, H-5), 5.11 (1H, d, J = 4.8 Hz, H-6) and 5.05 (1H, d, J = 10.8 Hz, H-8), δ_C 75.7 (C-5), 71.5 (C-6) and 76.9 (C-8), and two isobutyloxy groups. The spin systems inferred from the ^{1}H−^{1}H COSY spectrum (Fig. 4a), H_3-14/H-

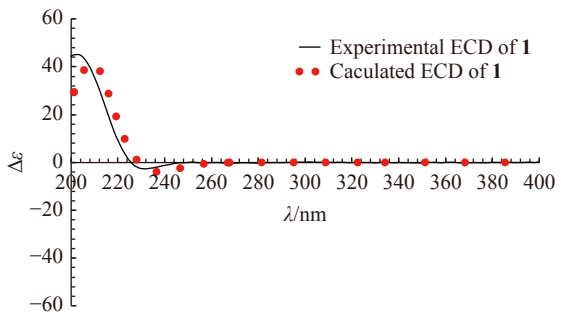

Fig. 3 Comparison of the experimental ECD and calculated ECD spectra of 1

10/H_2-1/H_2-2/H_2-3 and H-5/H-6/H-7/H-8, together with the HMBC correlations from H_3-14 (δ_H 1.29) to C-1 (δ_C 32.1), C-9 (δ_C 210.4), and C-10 (δ_C 44.7), from H_3-15 (δ_H 1.10) to C-3 (δ_C 35.4), C-4 (δ_C 74.3) and C-5 (δ_C 75.7), from H-5 (δ_H 4.87) to C-6 (δ_C 71.5) and C-1" (δ_C 176.3), and from H-8 (δ_H 5.05) to C-6 (δ_C 71.5), C-7 (δ_C 45.6), C-9 (δ_C 210.4), C-10 (δ_C 44.7), and C-1' (δ_C 175.5), revealed that compound **3** contained a 10-membered ring with Me-14 located at C-10, Me-15 at C-4 and two isobutyloxy groups at C-5, C-8 respectively. Moreover, the *α*-methylene-*γ*-lactone was established from the HMBC correlations of H-7/C-12, H_2-13/C-11, and H_2-13/C-12. The ROESY association of H-5 (δ_H 4.87) to H-7 (δ_H 3.41), H-5 (δ_H 4.87) to Me-15 (δ_H 1.10), H-8 (δ_H 5.05) to H-10 (δ_H 3.12) and H-6 (δ_H 5.11) to H-8 (δ_H 5.05) indicated that H-6, H-8, and H-10 were *β*-oriented while H-5, H-7, and Me-15 were *α*-oriented. These observations revealed that **3** closely resembled incaspitolide A [16-17]. The only structural difference was the orientation of Me-14. The *α*-orientation of Me-14 was proposed based on the ROESY association between H-10 (δ_H 3.12) and H-6 (δ_H 5.11; Fig. 4b). The structure of **3**, carpescernolide E was thus determined as 5, 8-di(isobutyloxy)-4-hydroxy-9-oxogermacran-6, 12-olide.

The six known compounds, namely incaspitolide A (**4**) [17-18], ineupatolide (**5**) [19-20], ineupatolides E (**6**) [15], 2*β*, 5-epoxy-5, 10-dihydroxy-6*α*-angeloyloxy-9-isobutyloxy-germacran-8*α*, 12-olide (**7**) [21], 4E-9*β*-hydroxy-7*α*, 10*α*H-germacra-4, 11(13)-dien-12, 6*α*-olide (**8**) [22], and 11(13)-dehydroivaxillin (**9**) [23-24], were established by NMR and comparison with literature values.

Anti-leukemia activity

Germacranolide sesquiterpenes exhibit toxicity against leukemia cell lines. To investigate the anti-leukemia activity of the compounds separated from *C. cernuum*, HEL, K562 and KG-1a cells were exposed to these compounds at 10 μmol·L^{-1} for 72 h (Fig. 5). Compounds **1**–**3** and compound **7** showed significant activity towards HEL, KG-1a and K562 cells. Furthermore, compounds **4** and **5** showed the highest activity among the nine compounds towards HEL cells, and no activity was seen towards K562 cells. Compound **9** was active to HEL cells alone. Compounds **6** and **8** had no activity towards any of the leukemia cells. To determine the IC_{50} of the active compounds, HEL, K562 and KG-1a cells were treated with these compounds and imatinib at different concentrations for 72 h (Table 3). In general, compounds **1**–**3** were more active than compounds **4**–**9**. Compounds **1**–**5** and **7** showed greater activity than imatinib on HEL cells. Among compounds **1**–**5**, **2** and **3** showed better cytotoxic effects on HEL and K562 cells. Therefore, they were both subjected to apoptotic flow cytometry using HEL and K562 cells.

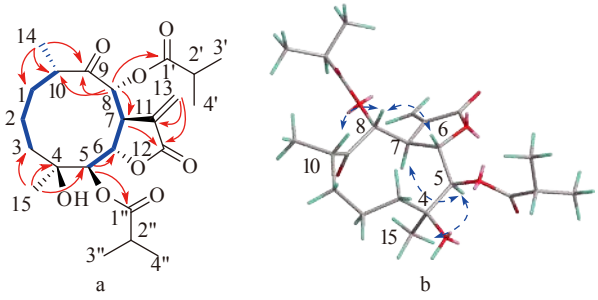

Fig. 4 (a) Key HMBC (H→C) and ^{1}H–^{1}H COSY (—) correlations of 3; (b) Selected ROESY correlations (H↔H) of 3

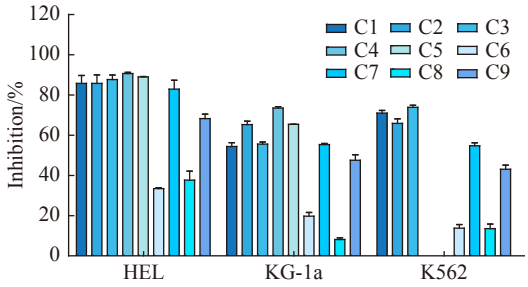

Fig. 5 The inhibition rate of compounds (C1–C9) at 10 μmol·L^{-1} for 72 h. Data are represented as mean ± SD, and values were averaged from at least three independent experiments

*Compounds **2** and **3** induce apoptosis in HEL and K562 cells*

Flow cytometry results showed that compounds **2** and **3** significantly induced apoptosis in HEL and K562 cells in a dose dependent manner (Fig. 6), indicating their role as potential anti-cancer agents. Compound **2** showed similar apoptotic rates in both cell lines. According to previous research, MTT assay is suitable to investigate mitochondrial apoptosis pathways [25], which suggested cell apoptosis was induced by other pathways other than the mitochondrial pathway. Therefore, Western blot was conducted on K562 cells using compound **2**.

*Effects of compound **2** on apoptotic proteins in K562 cells*

K562 cells were treated with different concentrations of **2** for 24 h, and the levels of apoptotic-related proteins were analyzed. The results showed that pro-apoptotic proteins caspase 9 and PARP were activated in a dose-dependent manner while the expression of anti-apoptotic proteins Bcl-2, NF-*κ*B

Table 3 The IC_{50} values of the active compounds against HEL, KG-1a and K562 cell lines (mean ± SD, n = 3)

Compounds	72 h IC_{50}/(μmol·L^{-1})		
	HEL	KG-1a	K562
1	2.01 ± 0.21**	5.47 ± 0.66**	3.27 ± 0.71**
2	2.48 ± 0.80*	5.21 ± 1.21*	3.75 ± 0.52*
3	1.59 ± 1.20**	5.28 ± 0.52**	2.26 ± 0.23**
4	1.17 ± 0.54**	4.45 ± 0.55**	> 10
5	2.34 ± 0.78*	7.24 ± 0.18*	> 10
7	2.60 ± 2.11*	6.34 ± 0.59*	5.94 ± 1.34*
9	6.90 ± 0.70*	> 10	> 10
Imatinib	4.24 ± 0.04	3.51 ± 0.22	0.09 ± 0.01

IC_{50} values were assayed by MTT with different concentrations of the active compounds. *P < 0.05 and **P < 0.01 *vs* the control group, respectively

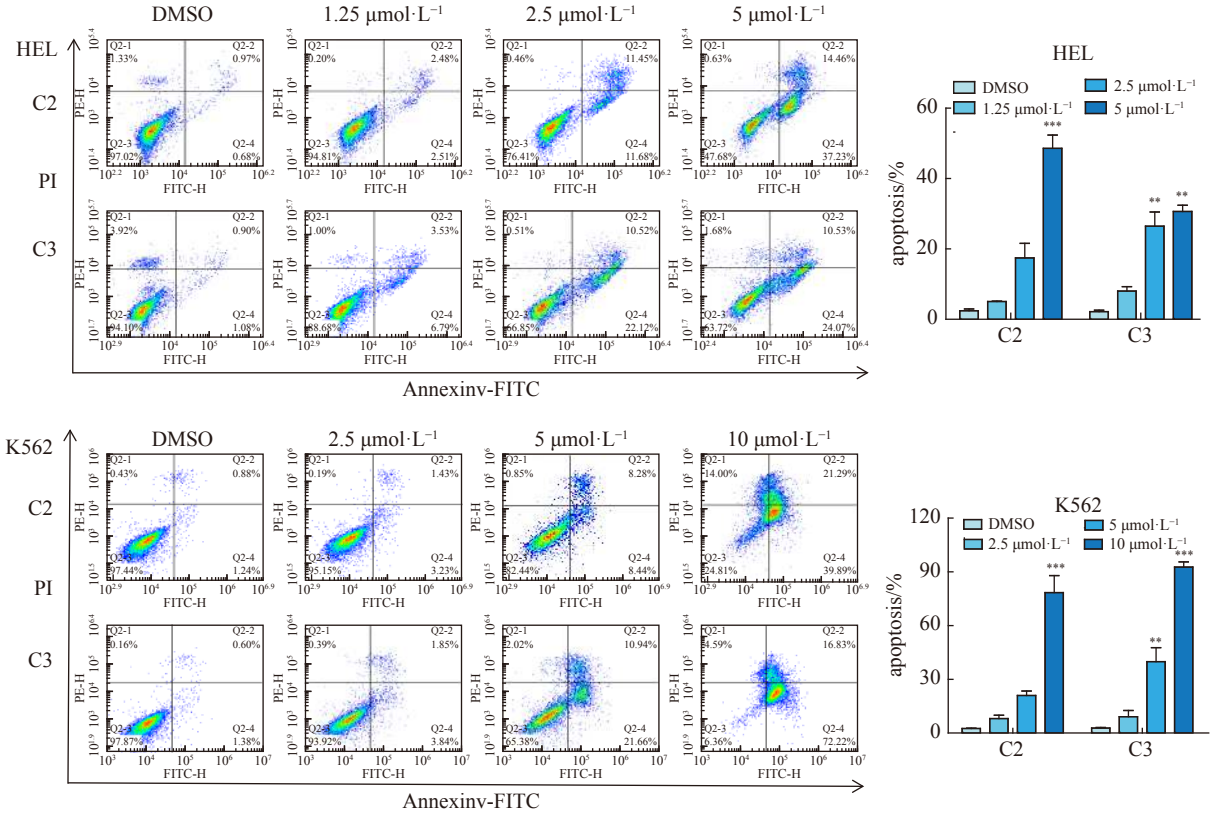

Fig. 6 Compounds 2 and 3 induce apoptosis in HEL and K562 cells. (A) HEL cells were treated with 2 and 3 at 0, 1.25, 2.5, and 5 μmol·L^{-1} for 24 h. The highest apoptosis rate reached about 50%. (B) K562 cells were treated with 2 and 3 at 0, 2.5, 5, and 10 μmol·L^{-1} for 24 h. The highest apoptosis rate reached about 90%. Data are represented as mean ± SD (n = 3). $^{*}P < 0.05$, $^{**}P < 0.01$, $^{***}P < 0.001$ *vs* control

and survivin decreased (Fig. 7). The caspase family is vital for apoptosis induction [26] and in the current study, caspase 9 was activated. However, compound **2** produced increased effects on the anti-apoptotic protein Bcl-2 related to mitochondrial apoptosis [27]. These findings are consistent with previous studies and indicated that alternative apoptosis mechanisms may be responsible for the death of K562 cells. Previous works have demonstrate that increased PARP cleavage makes DNA repair dysfunctional and induces K562 cell apoptosis [28]. In a similar manner, the expression of full-length PARP significantly decreased using **2**, suggesting cellular apoptosis. A sesquiterpene lactone isolated from the *Saussurea lappa* costunolide showed apoptosis towards SK-MES-1 human lung squamous carcinoma cells. That lactone also showed dose-dependent morphological alterations and inhibited cell cycles during the G_1/S phase. The Bax was up-regulated and Bcl-2 was down-regulated by costunolide treatment [29], which was similar to the action of compound **2** on K562 cells. This Bcl-2 activation eventually caused caspase-3 activation and costunolide-induced apoptosis. Treatments with compound **2** even resulted in caspase 3 activation on K562 cells. However, another dimer sesquiterpene lactone isolated from *Smallanthus sonchifolius* induced G_2/M arrest and apoptosis by a mitochondrial pathway in HeLa cells [30].

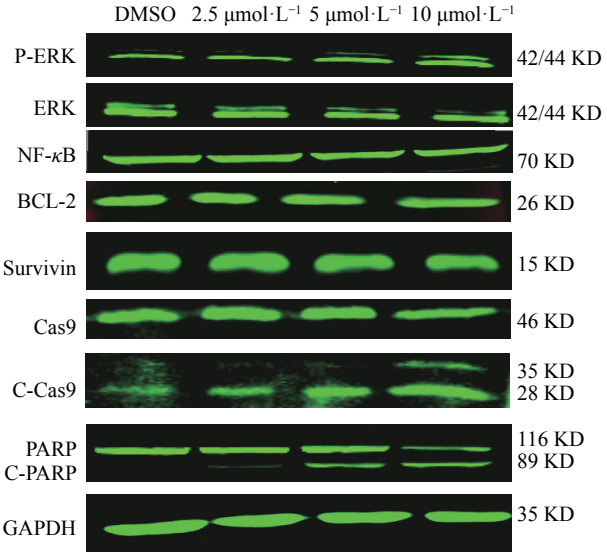

Fig. 7 Apoptotic proteins were analyzed by Western blot. Bcl-2, NF-NF-κB and Survivin were mildly inhibited. The caspase family and PARP were activated and P-ERK increased

We also investigated the effects of compound **2** on the upstream protein ERK. ERK belongs to the MAPK family and the MARK/ERK signaling pathway is necessary for various cellular responses, such as mitosis, differentiation, sur-

vival, migration and apoptosis during vertebrate embryonic development [31-32]. In most cancers, ERK is highly activated, resulting in physiological homeostasis imbalance [33]. ERK activation promotes both intrinsic/extrinsic pathways, which may result from caspase activation through permanent cell cycle arrest or autophagic vacuolization. These events require constant subcellular ERK phosphorylation and we observed a dose-dependent elevation in the p-ERK expression by compound **2**. In another study, helenalin, a cell-permeable pseudoguainolide sesquiterpene lactone, increased pERK levels in a concentration-dependent manner in HL-60 cells and caused MAPK activation [30]. This finding confirmed the role of **2** in apoptosis.

Conclusion

In the present study, a novel series of germacranolide sesquiterpene compounds are separated from the *C. cernuum,* which show anti-leukemia activity in human leukemia cell lines through activating Bcl-2 and causing cell cycle arrest. Moreover, this study demonstrates that these compounds may kill leukemia cells by inducing apoptosis through the activation of ERK.

Experimental

General Experimental Procedures

Optical rotations were measured with a JASCO P-1020 polarimeter (Jasco , Tokyo, Japan). UV spectra's were recorded on a Shimadzu UV-2401A (Shimadzu, Kyoto, Japan). ECD spectra's were recorded with an Applied Photophysics Chirascan spectrometer (Berlin, Germany). IR spectra's were determined on a Bruker Tensor-27 infrared spectrophotometer with KBr disks (bruker optics, germany). ^{1}H and ^{13}C NMR and 2D NMR spectra's were recorded on an INOVA-400 MHz (VARIAN, USA) with tetramethylsilane (TMS) as an internal standard. Bruker HCT/E Squire (Bruker, USA) and Waters Autospec Premier P776 mass spectrometers (Waters, USA) were used to measure ESIMS and HR-EIMS, respectively. Semipreparative HPLC was performed on a Waters 1525 liquid chromatograph with a Waters XBridge C_{18} (4.6 mm × 150 mm; 10 mm × 250 mm, 5 μm) column (Waters, USA). Column chromatography (CC) was performed using silica gel (200–300 mesh and 300–400 mesh, Qingdao Marine Chemical, Inc., Qingdao, China). TLC spots were visualized under UV light (ZF-6, JIAPENG echnology Co., Ltd, Shanghai, China) and by dipping into 5% H_2SO_4 in EtOH followed by heating (Analytical reagent, energy-chemical, Shanghai, China).

Plant material

The whole plant of *C. cernuum* was collected in Zhenning, Guizhou Province, China, and identified by Professor SUN Qing-Wen of Guiyang College of Traditional Chinese Medicine. A voucher specimen (Assrmyy201608) was deposited at pharmacy's comprehensive laboratory of Anshun City People's Hospital.

Extraction and isolation

The powder of an entire plant of dried *C. cernuum* (20.0 kg) was extracted with 95% EtOH (20 L × 3; 80 °C for 3 h). The residue suspended in water was extracted with EtOAc and the resultant extract (960.0 g) was subjected to column chromatography over 3 kg of silica gel (15 cm × 160 cm, 300–400 mesh) and eluted with a gradient of petroleum ether−acetone (from 60 : 1 to 0 : 1, *V/V*) to give 7 fractions (Fr.1–7). Fr. 5 (82.0 g) was chromatographed on a silica gel column (petroleum ether–EtOAc from 9 : 1 to 5 : 5, *V/V*) to give sub-fractions 5a−5e. Sub-fraction 5b was purified by Sephadex LH-20 ($CHCl_3$−MeOH, 1 : 1, *V/V*) and chromatographed on a C_{18} silica gel column (MeOH−H_2O, 4 : 6 to 7 : 3, *V/V*) to obtain **3** (10.3 mg), **5** (55.4 mg) and **8** (9.6 mg). Sub-fraction 5c was fractionated on a Sephadex LH-20 column (MeOH) and recrystallized to obtain compound **6** (10.5 mg). Sub-fraction 5d was further eluted on a C_{18} silica gel column (MeOH−H_2O, 7 : 3, *V/V*) to afford compounds **7** (19.6 mg) and **9** (8.3 mg). Sub-fraction 5e was subjected to CC over silica gel (petroleum ether–ethyl acetate from 9 : 1 to 8 : 2, *V/V*) to obtain three fractions, which were then separated using a Waters X-Bridge C_{18} column (SunFire®C_{18}, 5 μm, 4.6 mm × 250 mm, MeCN−H_2O, 50 : 50, *V/V*) to afford **1** (9.5 mg), **2** (8.6 mg) and **4** (32.6 mg).

Compound characterization data

Carpescernolide C (**1**): White amorphous powder; $[\alpha]_D^{20}$ (*c* 0.40, MeOH); UV (MeOH) λ_{max} (log ε) m 197 (1.64); IR (KBr) ν_{max} 3439, 2975, 2931, 1768, 1754, 1633, 1459, 1384, 1161, 993 cm^{-1}; ^{1}H and ^{13}C NMR data see Table 1; positive ESIMS *m/z* 389 $[M + Na]^+$; HR-ESIMS *m/z* 389.1570 $[M + H]^+$ (Calcd. for $C_{19}H_{27}O_7$, 389.1571).

Carpescernolide D (**2**): White amorphous powder; $[\alpha]_D^{20}$ 43.33 (*c* 0.80, MeOH); UV (MeOH) λ_{max} (log ε) m 205 (2.64); IR (KBr) ν_{max} 3427, 2995, 2936, 1768, 1767, 1635, 1459, 1382, 1251, 1137, 1046, 968 cm^{-1}; ^{1}H and ^{13}C NMR data see Table 1; positive ESIMS *m/z* 381 $[M + H]^+$; HR-ESIMS *m/z* 403.1725 $[M + Na]^+$ (Calcd. for $C_{20}H_{28}O_7Na$, 403.1727).

Carpescernolide E (**3**): White amorphous powder; $[\alpha]_D^{20}$ −37.78 (*c* 0.30, MeOH); UV (MeOH) λ_{max} (log ε) m 195 (2.79); IR (KBr) ν_{max} 3444, 2996, 2924, 1773, 1762, 1639, 1457, 1274, 990 cm^{-1}; ^{1}H and ^{13}C NMR data see Table 1; positive ESIMS *m/z* 439 $[M + H]^+$; HR-ESIMS m/z 461.2147 $[M + Na]^+$ (Calcd. for $C_{23}H_{34}O_8Na$, 461.2146).

Anti-leukemia assays

Cell lines

Human leukemia cell lines HEL, K562 and KG-1a were obtained from ATCC, Manassas, VA, USA, and cultured in RPMI 1640 medium (Giboc, USA) supplemented with 5% fetal bovine serum (VACCA, USA) at 37 °C, 95% humidity and 5% CO_2.

MTT assay

Leukemia cell lines HEL, K562 and KG-1a were seeded in 96-well plates at densities between (4×10^3)–(1×10^4) and treated with various concentrations of chemical agents after 24 h. They were incubated for 72 h and 10 μL of MTT

(5 mg·mL^{-1}) was added to each well before incubation for an additional 4 h and centrifugation at 3000 r·min^{-1} for 20 min. DMSO (160 μL) was added to each well after the supernatant was discarded. The absorbance of the formazan products was measrued at 490 nm using a Synergy2 modular Multi-Mode Reader (BioTek, Winooski, VT, USA) [34-35].

Cell apoptosis assay

Apoptosis was assessed after the cells (1.0 × 10^5/mL) were seeded in 6-well plates and treated with different concentrations of the compounds for 24 h. The cells were then collected with microcentrifuge tubes, washed twice with precooling phosphate-buffered saline (PBS), resuspended for 20 min at room temperature in 50 μL 1× binding buffer, 2.5 μL FITC Annexin V (Becton, Dickinson, USA), and 2.5 μL propidium iodide (Becton, Dickinson, USA) for flow cytometry [34].

Western blot analysis

The cells were seeded in 60 × 60 dishes and treated with compound **2** for 24 h. Protein samples (30 μg) were separated by 10% or 12% SDS-PAGE with 100 V for approximately 120 min, electroblotted onto a PVDF membrane (0.22 μmol·L^{-1}, Bio-Rad, USA) at 220 mA for about 120 min and blocked with 3% bovine serum albumin (BSA) for 1 h at room temperature. The blocked membrane was subsequently incubated overnight at 4 °C with specific primary antibodies: Bcl-2 (abcam), caspase3 (CST), caspase 9 (CST), PARP (CST), survivin (CST), NF-*κ*B (CST), ERK (CST) and p-erk (CST). After washing three times with TBS for 15 min, the membrane was incubated for 1.5 h at room temperature with secondary FITC-anti-rabbit antibody (CST). The membrane was scanned using an infrared imaging scanner. GAPDH was used as the loading control [36].

Supplementary Information

Supporting information of this paper can be available on request from the corresponding authors.

References

[1] Zhang JP, Wang GW, Tian XH, *et al*. The genus *Carpesium*: A review of its ethnopharmacology, phytochemistry and pharmacology [J]. *J Ethnopharmacol*, 2015, **163**(1): 173-191.

[2] Yang YX, Shan L, Liu QX, *et al*. Carpedilactones A–D, four new isomeric sesquiterpene lactone dimers with potent cytotoxicity from *Carpesium faberi* [J]. *Org Lett*, 2014, **16**(16): 4216-4219.

[3] Liu QX, Yang YX, Zhang JP, *et al*. Isolation, structure elucidation, and absolute configuration of highly oxygenated germacranolides from *Carpesium cernuum* [J]. *J Nat Prod*, 2016, **79**(10): 2479-2486.

[4] Zhu NL, Tang CP, Xu CH, *et al*. Cytotoxic germacrane-type sesquiterpene lactones from the whole plant of *Carpesium lipskyi* [J]. *J Nat Prod*, 2019, **82**(4): 919-927.

[5] Zong H, Sen S, Zhang G, *et al*. *In vivo* targeting of leukemia stem cells by directing parthenolide-loaded nanoparticles to the bone marrow niche [J]. *Leukemia*, 2016, **30**(7): 1582-1586.

[6] Siveen KS, Uddin S, Mohammad RM. Targeting acute myeloid leukemia stem cell signaling by natural products [J]. *Mol Cancer*, 2017, **16**(1): 13.

[7] Bali EB, Açık L, Elçi P, *et al*. *In vitro* anti-oxidant, cytotoxic and pro-apoptotic effects of achillea teretifolia willd extracts on human prostate cancer cell lines [J]. *Pharmacogn Mag*, 2015, **11**(2): 308-315.

[8] Robles AJ, Peng J, Hartley RM, *et al*. Melampodium leucanthum, a source of cytotoxic sesquiterpenes with antimitotic activities [J]. *J Nat Prod*, 2015, **78**(3): 388-395.

[9] Ashtiani M, Nabatchian F, Galavi HR, *et al*. Effect of Achillea wilhelmsii extract on expression of the human telomerase reverse transcriptase mRNA in the PC3 prostate cancer cell line [J]. *Biomed Rep*, 2017, **7**(3): 251-256.

[10] Shaffer CV, Cai S, Peng J, *et al*. Texas native plants yield compounds with cytotoxic activities against prostate cancer cells [J]. *J Nat Prod*, 2016, **79**(3): 531-540.

[11] Niu JX, Huang H, Wang F, *et al*. Synthetic derivatives of the natural product 13-amino 2-desoxy-4-epi-pulchellin inhibit STAT3 signaling and induce G_2/M arrest and death of colon cancer cells [J]. *Bioorg Med Chem Lett*, 2019, **29**(6): 782-785.

[12] Dang H, Li H, Ma C, *et al*. Identification of *Carpesium cernuum* extract as a tumor migration inhibitor based on its biological response profiling in breast cancer cells [J]. *Phytomedicine*, 2019, **64**: 153072.

[13] Ahn EY, Jin H, Park Y. Green synthesis and biological activities of silver nanoparticles prepared by *Carpesium cernuum* extract [J]. *Pharm Res*, 2019, **42**(10): 926-934.

[14] Yan C, Zhang WQ, Sun M, *et al*. Carpescernolides A and B, rare oxygen bridge-containing sesquiterpene lactones from *Carpesium cernuum* [J]. *Tetrahedron Lett*, 2018, **59**(46): 4063-4066.

[15] Wu JW, Tang CP, Cai YY, *et al*. Cytotoxic germacrane-type sesquiterpene lactones from the whole plant of *Inula cappa* [J]. *Chin Chem Lett*, 2017, **28**(5): 927-930.

[16] Gonzalez AG, Bermejo J, Triana J, *et al*. Sesquiterpene lactones and other constituents of *Allagopappus* species [J]. *J Nat Prod*, 1995, **58**(3): 432-437.

[17] Zhang T, Si JG, Zhang QB, *et al*. New highly oxygenated germacranolides from *Carpesium divaricatum* and their cytotoxic activity [J]. *Sci Rep*, 2016, **6**: 27237.

[18] Bohlmann F, Singh P, Jakupovic J. Further ineupatorolide-like germacranolides from *Inula cuspidata* [J]. *Phytochemistry*, 1981, **20**(1): 1883-1885.

[19] Baruah RN, Sharma RP, Thyagarajan G. Unusual germacranolides from *Inula eupatorioides* [J]. *J Org Chem*, 1980, **45**(24): 4838-4843.

[20] Baruah NC, Baruah RN, Sharma RP, *et al*. Germacranolides of *Inula eupatorioides*. 2. Absolute configuration of the ineupatorolides [J]. *J Org Chem*, 1982, **47**(1): 137-140.

[21] Kim DK, Lee KR, Zee OP. Sesquiterpene lactones from *Carpesium divaricatum* [J]. *Phytochemistry*, 1997, **46**(7): 1245-1247.

[22] Cheng XR, Zhang SD, Wang CH, *et al*. Bioactive eudesmane and germacrane derivatives from *Inula wissmanniana* Hand. Mazz [J]. *Phytochemistry*, 2013, **96**: 214-222.

[23] Wang F, Yang K, Ren FC, *et al*. Sesquiterpene lactones from *Carpesium abrotanoides* [J]. *Fitoterapia*, 2009, **80**(1): 21-24.

[24] Maruyama M, Karube A, Sato K. Sesquiterpene lactones from *Carpesium abrotanoides* [J]. *Phytochemimy*, 1983, **22**(12): 2773-2774.

[25] Rai Y, Pathak R, Kumari N, *et al*. Mitochondrial biogenesis and metabolic hyperactivation limits the application of MTT assay in the estimation of radiation induced growth

inhibition [J]. *Sci Rep*, 2018, **8**(1): 1531.
[26] Fuchs Y, Steller H. Live to die another way: modes of programmed cell death and the signals emanating from dying cells [J]. *Nat Rev Mol Cell Biol*, 2015, **16**(6): 329-344.
[27] Baig S, Seevasant I, Mohamad J, *et al*. Potential of apoptotic pathway-targeted cancer therapeutic research: where do we stand? [J]. *Cell Death Dis.*, 2016, **7**(1): e2058.
[28] Curtin NJ, Szabo C. Therapeutic applications of PARP inhibitors: anticancer therapy and beyond [J]. *Mol Aspects Med*, 2013, **34**(6): 1217-1256.
[29] Hua P, Zhang G, Zhang Y, *et al*. Costunolide induces G_1/S phase arrest and activates mitochondrial-mediated apoptotic pathways in SK-MES 1 human lung squamous carcinoma cells [J]. *Oncol Lett*, 2016, **11**(4): 2780-2786.
[30] Kim SH, Oh SM, Kim TS. Induction of human leukemia HL-60 cell differentiation *via* a PKC/ERK pathway by helenalin, a pseudoguainolide sesquiterpene lactone [J]. *Eur J Pharmacol*, 2005, **511**(2-3): 89-97.
[31] Gotoh Y, Moriyama K, Matsuda S, *et al*. Xenopus M phase MAP kinase: isolation of its cDNA and activation by MPF [J]. *EMBO J*, 1991, **10**(9): 2661-2668.
[32] Mebratu Y, Tesfaigzi Y. How ERK1/2 activation controls cell proliferation and cell death is subcellular localization the answer? [J]. *Cell Cycle*, 2009, **8**(8): 1168-1175.
[33] Maik-Rachline G, Hacohen-Lev-Ran A, Seger R. Nuclear ERK: Mechanism of translocation, substrates, and role in cancer [J]. *Int J Mol Sci*, 2019, **20**(5): E1194.
[34] Wang N, Fan Y, Yuan CM, *et al*. Selective ERK1/2 agonists isolated from *Melia azedarach* with potent anti-leukemic activity [J]. *BMC Cancer*, 2019, **19**(1): 764.
[35] Gajendran B, Durai P, Varier KM, *et al*. Green synthesis of silver nanoparticle from *Datura inoxia* flower extract and its cytotoxic activity [J]. *BioNanoScience*, 2019, **9**(3): 564-572.
[36] Song J, Yuan C, Yang J, *et al*. Novel flavagline-like compounds with potent Fli-1 inhibitory activity suppress diverse types of leukemia [J]. *FEBS J*, 2018, **285**(24): 4631-4645.

Cite this article as: YAN Chen, LONG Qun, ZHANG Yun-Dong, BABU Gajendran, KRISHNAPRIYA Madhu Varier, QIU Jian-Fei, SONG Jing-Rui, RAO Qing, YI Ping, SUN Mao, LI Yan-Mei. Germacranolide sesquiterpenes from *Carpesium cernuum* and their anti-leukemia activity [J]. *Chin J Nat Med*, 2021, **19**(7): 528-535.